Electronic Supplementary Material (ESI) for Nanoscale.
This journal is © The Royal Society of Chemistry 2017

Supplementary Information

Rational Design of Super-alkalis and Their Role in CO_2 Activation

Tianshan Zhao[a, b], Qian Wang[a*], and Puru Jena[b*]

[a]Center for Applied Physics and Technology, College of Engineering, Peking University, Key Laboratory of High Energy Density Physics Simulation, and IFSA Collaborative Innovation Center, Ministry of Education, Beijing 100871, China.

[b]Department of Physics, Virginia Commonwealth University, Richmond, VA 23284

Correspondence to: qianwang2@pku.edu.cn, and pjena@vcu.edu

Supplementary Text 1. Detail electron configuration of $Mn(B_3N_3H_6)_2^+$ cation:

In the $Mn(B_3N_3H_6)_2^+$ cation the α-spin electron configurations of each H, B, N, and Mn atoms are $1s^{0.41}$, $2s^{0.61}2p^{0.74}$, $2s^{0.69}2p^{2.39}$ and $4s^{0.06}3d^{4.88}$, respectively, while the corresponding electron configurations of β-spin are $1s^{0.41}$, $2s^{0.30}2p^{0.79}$, $2s^{0.69}2p^{2.36}$ and $4s^{0.05}3d^{0.88}$, respectively.

Supplementary Text 2. Detail electron configuration of $B_9C_3H_{12}^+$ cation:

In the $B_9C_3H_{12}^+$ cation the electron configurations of each H, B, and C are $1s^{0.85}$, $2s^{0.66}2p^{2.17}$, and $2s^{1.03}2p^{3.66}$, respectively. This means that H and B atoms lose 0.15 and 0.17 electrons while C atom gains about 0.69 electrons.

Supplementary Text 3. Nucleus-independent chemical shift (NICS) criterion of Pyridine-H^+:

In order to confirm the stability of organic molecule, we calculated the nucleus-independent chemical shifts (NICS). Due to its simplicity and efficiency the NICS criterion[1] is an effective probe of aromaticity, consistent with the Hückel's rule.[1] NICS is typically computed at ring centers, at points above, and even as grids in and around the molecule. Significantly, negative NICS values in the interior positions of rings indicate the presence of induced diatropic ring currents or "aromaticity", whereas positive values at each point denote paratropic ring currents and "antiaromaticity". Several NICS indices are in common use, and because the NICS is a tensor, different components of the tensor are considered as appropriate indices of aromaticity.[2] In our study, we calculated NICS at the ring center (NICS(0)) and 1 Å above the ring center (NICS(1)). We find that the NICS(0) and NICS(1) are -7.78 and -9.34 which confirm Pyridine-H^+'s aromaticity.

Supplementary Text 4. Electron localization function (ELF) analyses of Pyridine-H^+:

Electron localization function (ELF) slices have also been calculated in the Pyridine-H^+ plane (ELF(0)) and 1 Å above the plane (ELF(1)), showing the localized σ band feature in ELF(0) and delocalized π bond feature in ELF(1). Results are given in Figs. S6 (a) and (b).

Supplementary Text 5. Detail electron configuration of Pyridine-H^+ cation:

In the Pyridine-H^+ cation the electron configurations of each H, C, and N are $1s^{0.71}$, $2s^{0.96}2p^{3.06}$, and $2s^{1.26}2p^{4.26}$, respectively. This means that H atom loses 0.29 electrons, while N atom gains about 0.52 electrons.

Supplementary Text 6. Detail electron configuration of $Mn(B_3N_3H_6)_2$ neutral cluster: In neutral $Mn(B_3N_3H_6)_2$ the α-spin electron configurations of each H, B, N, and Mn atoms are $1s^{0.42}$, $2s^{0.29}2p^{0.74}$, $2s^{0.68}2p^{2.39}$ and $4s^{0.10}3d^{4.71}$, respectively, while the corresponding electron configurations of β-spin are $1s^{0.41}$, $2s^{0.30}2p^{0.98}$, $2s^{0.67}2p^{2.30}$ and $4s^{0.18}3d^{1.52}$, respectively.

Supplementary Text 7. Detail electron configurations of $Mn(B_3N_3H_6)_2$ absorbed CO_2: When the CO_2 is adsorbed, the α-spin electron configurations of H, B, N, and Mn atoms become $1s^{0.41}$, $2s^{0.30}2p^{0.74}$, $2s^{0.68}2p^{2.38}$ and $4s^{0.08}3d^{4.23}$, respectively, in neutral $Mn(B_3N_3H_6)_2$ while the electron configurations of C and O are $2s^{0.58}2p^{1.31}$ and $2s^{0.88}2p^{2.60}$ in CO_2. The corresponding electron configurations of β-spin are $1s^{0.41}$, $2s^{0.31}2p^{0.76}$, $2s^{0.68}2p^{2.37}$ and $4s^{0.07}3d^{2.06}$ in $Mn(B_3N_3H_6)_2^+$ and $2s^{0.33}2p^{0.81}$ and $2s^{0.87}2p^{2.52}$ in CO_2, respectively.

Supplementary Text 8. Detail electron configuration of $B_9C_3H_{12}$ neutral cluster:
In neutral $B_9C_3H_{12}$, the α-spin electron configurations of each H, B, and C atoms are $1s^{0.45}$, $2s^{0.32}2p^{1.13}$, and $2s^{0.53}2p^{1.96}$, respectively, while the corresponding electron configurations of β-spin are $1s^{0.45}$, $2s^{0.32}2p^{1.09}$, and $2s^{0.51}2p^{1.76}$, respectively.

Supplementary Text 9. Detail electron configurations of $B_9C_3H_{12}$ absorbed CO_2:
When CO_2 is adsorbed, the α-spin electron configurations of H, B, and C atoms are $1s^{0.43}$, $2s^{0.33}2p^{1.09}$, and $2s^{0.52}2p^{1.83}$ in $B_9C_3H_{12}$ and the electron configurations of C and O are $2s^{0.61}2p^{1.32}$ and $2s^{0.89}2p^{2.59}$ in CO_2. The corresponding electron configurations of β-spin are $1s^{0.43}$, $2s^{0.33}2p^{1.09}$, and $2s^{0.52}2p^{1.83}$ in $B_9C_3H_{12}$ and $2s^{0.37}2p^{0.81}$ and $2s^{0.89}2p^{2.50}$ in CO_2, respectively.

Supplementary Text 10. Detail electron configuration of Pyridine-H neutral cluster:

In neutral Pyridine-H, the α-spin electron configurations of each H, C, and N atoms are $1s^{0.38}$, $2s^{0.49}2p^{1.67}$, and $2s^{0.63}2p^{2.28}$, respectively, while the corresponding electron configurations of β-spin are $1s^{0.48}$, $2s^{0.47}2p^{1.50}$, and $2s^{0.62}2p^{2.13}$, respectively.

Supplementary Text 11. Detail electron configurations of Pyridine-H absorbed CO_2: When CO_2 is adsorbed, the α-spin electron configurations of H, C, and N atoms are $1s^{0.37}$, $2s^{0.48}2p^{1.56}$, and $2s^{0.69}2p^{2.09}$ in Pyridine-H and the electron configurations of C and O are $2s^{0.62}2p^{1.31}$ and $2s^{0.87}2p^{2.55}$ in CO_2. The corresponding electron configurations of β-spin are $1s^{0.37}$, $2s^{0.48}2p^{1.56}$, and $2s^{0.69}2p^{2.09}$ in Pyridine-H and $2s^{0.37}2p^{0.81}$ and $2s^{0.87}2p^{2.44}$ in CO_2, respectively.

Supplementary Figures

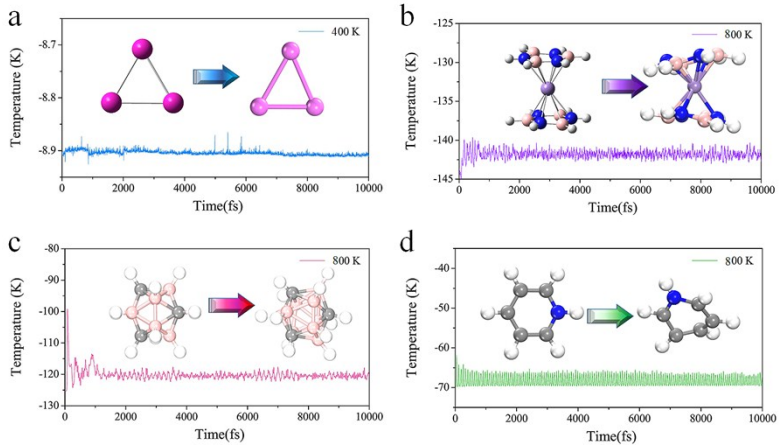

Figure S1. Thermodynamic stability of four different kinds of superalkalis, namely (a) Al_3^+, (b) $Mn(B_3N_3H_6)_2^+$, (c) $B_9C_3H_{12}^+$ and (d) Pyridine-H^+, studied using *ab initio* molecular dynamics simulation. The Nosé heat bath method[3] is adopted at a given temperature for 10 *ps* with 1 *fs* interval. The potential energy plots corresponding to the initial and final snap shots are given in Supplementary Figures 1a-d. During simulations only structural distortions are noticed, but the bonding, structures, and stabilities remain unaffected.

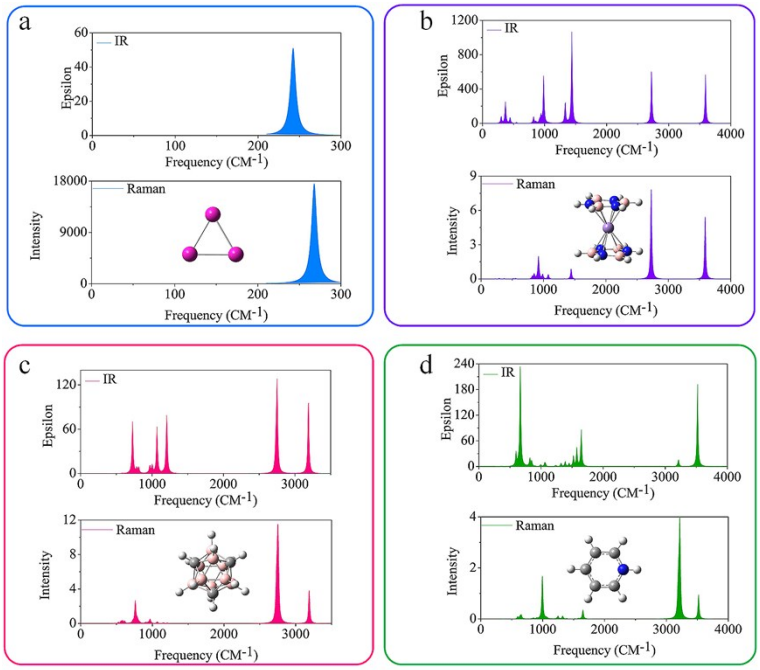

Figure S2. The IR and Raman spectra of four different kinds of superalkalis, namely (a) Al_3^+, (b) $Mn(B_3N_3H_6)_2^+$, (c) $B_9C_3H_{12}^+$ and (d) Pyridine-H^+ studied. The half-width at half height is 10 cm^{-1} in both IR and Raman spectra.

With regard to the IR spectroscopy, we found that the vibrational frequencies of Al_3^+ are mainly distributed in the 200 to 250 cm^{-1} region. The vibrational frequency distributions of $B_9C_3H_{12}^+$ are at 870, 1100, 1230, 2700, and 3200 cm^{-1}. The vibrational frequency distributions of Pyridine-H^+ are located at 600, 1600, and 3500 cm^{-1}. The vibrational frequency distributions of $Mn(B_3N_3H_6)_2^+$are at 430, 970, 1400, 2700, and 3600 cm^{-1}.

With regard to Raman spectroscopy, we found that the peak distribution is around 270 cm^{-1} in Al_3^+. The vibrational frequency distributions of $B_9C_3H_{12}^+$ are at 870, 2700, and 3300 cm^{-1}. The vibrational frequency distributions of Pyridine-H^+ are located at 1000 and 3200 cm^{-1}. The vibrational frequency distributions of $Mn(B_3N_3H_6)_2^+$are at 890, 2700, and 3600 cm^{-1}.

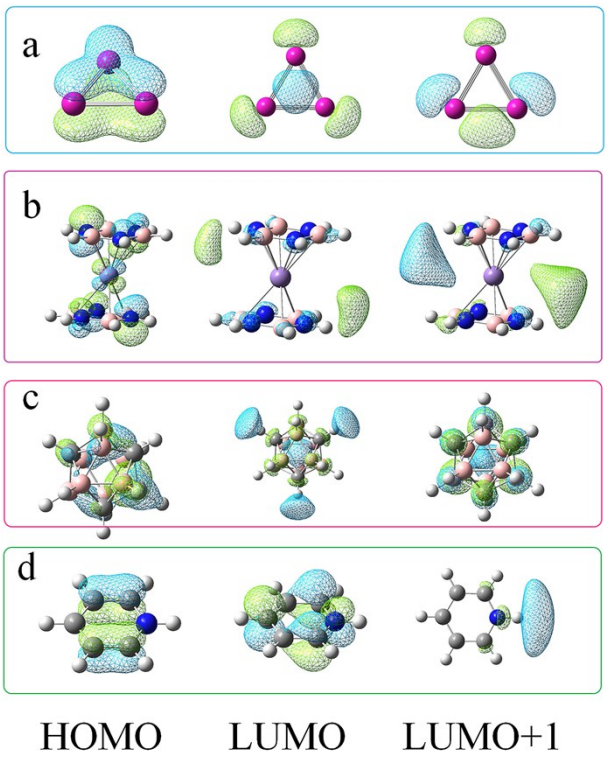

Figure S3. The HOMO, LUMO and LUMO+1 orbitals of four different kinds of cation namely (a) Al_3^+, (d) $Mn(B_3N_3H_6)_2^+$, (b) $B_9C_3H_{12}^+$, (c) Pyridine-H^+ and, respectively.

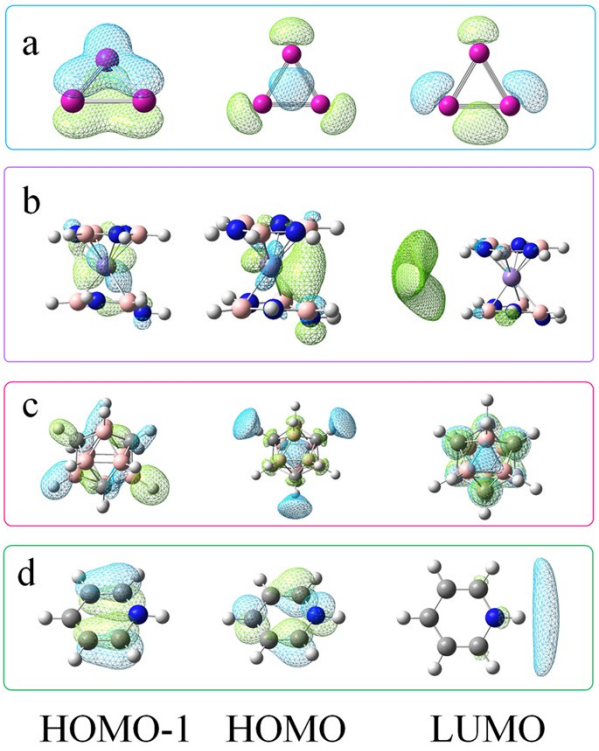

Figure S4. The HOMO-1, HOMO and LUMO orbitals of four different kinds of neutral molecules namely (a) Al_3, (b) $Mn(B_3N_3H_6)_2$, (c) $B_9C_3H_{12}$, and (d) Pyridine-H, respectively.

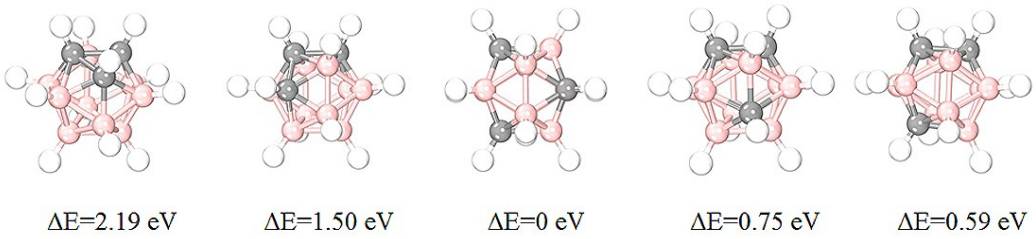

Figure S5. Optimized geometries of five different isomers of $B_9C_3H_{12}^+$ cation and their relative energies with respected the lowest energy configuration (1, 7, 9) $B_9C_3H_{12}^+$.

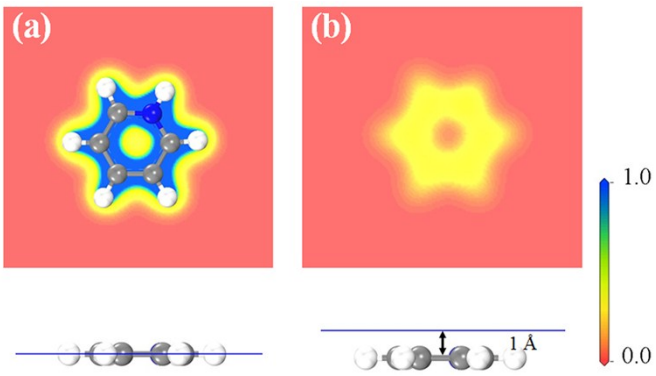

Figure S6. ELF(0) and ELF(1) slices of Pyridine-H^+ superalkali.

Supplementary Methods

The atomic structure optimizations, NICS, and vibrational frequency (IR and Raman) are calculated at the MP2 level.[4-6] Besides, single point calculations of molecular orbitals NBO analysis are carried out at the CCSD level of theory,[7, 8] with 6-311+G* basis set for all atom,[9] embedded in the Gaussian 09 code.[10] Frequency analysis was performed at the same level of theory to ensure that there are no imaginary frequencies and the structures belong to a minimum in the potential energy surface.

Thermodynamic stability, magnetic properties, and ELF analysis are carried out using density functional theory (DFT) as implemented in the Vienna Ab initio Simulation Package (VASP).[11] The projector augmented wave (PAW) method[12] and Perdew–Burke–Ernzerhof (PBE)[13] exchange correlation functional within generalized gradient approximation (GGA) are used. Plane waves with a kinetic energy cutoff of

500 eV are used to expand the valence electron wave functions. For all structural relaxations the convergence criteria for total energy and Hellmann–Feynman force are set to 10^{-4} eV and 10^{-2} eV $Å^{-1}$, respectively. A unit cell with a vacuum space of 30 Å in three directions is used in order to avoid virtual interactions. The first Brillouin zone is sampled by the Γ-point.[14] Ab initio molecular dynamics (AIMD) simulations are also performed to assess the thermal stability of the different Al_3^+, $B_9C_3H_{12}^+$, $C_5NH_6^+$ and $Mn(B_3N_3H_6)_2^+$cations. Canonical (NVT) ensemble is adopted using the Nosé heat bath method.[3]

The electron localization function (ELF) is a clear description of electron distribution in molecules,[15] which is used for chemical bond classification.[16] The ELF refers to the jellium-like homogeneous electron gas and renormalizes the value to between 0.0 and 1.0. The values of 1.0 and 0.5 correspond to fully localized and fully delocalized electrons, respectively, whereas the value 0.0 refers to nearly no charge density. We calculated the ELF of the Pyridine-H^+ cation to identify its bond character. Slices parallel in the ring plane are called ELF(0) and 1 Å above the ring plane called ELF(1). These are plotted in Fig. s6a and s6b, respectively.

To account for strong correlation of the unfilled *d* orbital of Mn-*d* atom, we apply the GGA+*U* scheme to account for the magnetic property of $Mn(B_3N_3H_6)_2$.[17] We carried out test calculations with effective *U* values ranging from 2 to 5 eV, and found that the magnetic moment of Mn is $4\mu_B$ and $3\mu_B$ in $Mn(B_3N_3H_6)_2^+$cation and $Mn(B_3N_3H_6)_2$ neutral, respectively, no matter which value of *U* adopted.

Supplementary References

1. E. Hückel, *Zeitschrift für Physik*, 1931, **70**, 204-286.
2. Z. Chen, C. S. Wannere, C. Corminboeuf, R. Puchta and P. v. R. Schleyer, *Chem. Rev.*, 2005, **105**, 3842-3888.
3. S. Nosé, *J. Chem. Phys.*, 1984, **81**, 511-519.
4. M. Head-Gordon, J. A. Pople and M. J. Frisch, *Chem. Phys. Lett.*, 1988, **153**, 503-506.
5. S. Sæbø and J. Almlöf, *Chem. Phys. Lett.*, 1989, **154**, 83-89.
6. M. J. Frisch, M. Head-Gordon and J. A. Pople, *Chem. Phys. Lett.*, 1990, **166**, 275-280.
7. G. D. Purvis and R. J. Bartlett, *J. Chem. Phys.*, 1982, **76**, 1910-1918.

8. G. E. Scuseria, C. L. Janssen and H. F. Schaefer, *J. Chem. Phys.*, 1988, **89**, 7382-7387.
9. M. J. Frisch, J. A. Pople and J. S. Binkley, *J. Chem. Phys.*, 1984, **80**, 3265-3269.
10. M. Frisch, G. Trucks, H. B. Schlegel, G. Scuseria, M. Robb, J. Cheeseman, G. Scalmani, V. Barone, B. Mennucci and G. Petersson, *Inc., Wallingford, CT*, 2009, **270**, 271.
11. G. Kresse and J. Furthmüller, *Phys. Rev. B*, 1996, **54**, 11169.
12. P. E. Blöchl, *Phys. Rev. B*, 1994, **50**, 17953-17979.
13. J. P. Perdew, K. Burke and M. Ernzerhof, *Phys. Rev. Lett.*, 1996, **77**, 3865.
14. H. J. Monkhorst and J. D. Pack, *Phys. Rev. B*, 1976, **13**, 5188-5192.
15. A. D. Becke and K. E. Edgecombe, *J. Chem. Phys.*, 1990, **92**, 5397-5403.
16. B. Silvi and A. Savin, *Nature*, 1994, **371**, 1808-1832.
17. S. L. Dudarev, G. A. Botton, S. Y. Savrasov, C. J. Humphreys and A. P. Sutton, *Phys. Rev. B*, 1998, **57**, 1505-1509.